P H Y S I C A L   R E V I E W   L E T T E R S

Critical Exponents of Strongly Correlated Fermion Systems from Diagrammatic Multiscale Methods

Andrey E. Antipov,[1,2,3,*] Emanuel Gull,[3,†] and Stefan Kirchner[1,2,‡]

[1]*Max Planck Institute for Chemical Physics of Solids, Nöthnitzer Straße 40, 01187 Dresden, Germany*
[2]*Max Planck Institute for the Physics of Complex Systems, Nöthnitzer Straße 38, 01187 Dresden, Germany*
[3]*Department of Physics, University of Michigan, Ann Arbor, Michigan 48109, USA*

Self-consistent dynamical approximations for strongly correlated fermion systems are particularly successful in capturing the dynamical competition of local correlations. In these, the effect of spatially extended degrees of freedom is usually only taken into account in a mean field fashion or as a secondary effect. As a result, critical exponents associated with phase transitions have a mean field character. Here we demonstrate that diagrammatic multiscale methods anchored around local approximations are indeed capable of capturing the non-mean-field nature of the critical point of the lattice model encoded in a nonvanishing anomalous dimension and of correctly describing the transition to mean-field-like behavior as the number of spatial dimensions increases.

Lattice models of correlated fermions appear in a wide variety of physical systems, from condensed matter, where they are used to study low-energy models of, e.g., transition metals and intermetallic rare earth and actinide compounds, to quantum chemistry and quantum chromodynamics. Many of these systems exhibit a plethora of phases that arise out of the dynamic competition of the underlying degrees of freedom. Understanding the possible orders that characterize these phases and the various ways they can disappear is of primary interest in current many-body physics.

The universal theory for the continuous melting of order at finite temperature applies to the 'scaling' regime in the immediate vicinity of the transition temperature T_c. Relating it to microscopic models of lattice fermions requires knowledge of the underlying universality class. Even for classical systems, identifying this universality class is difficult and relies, in general, on numerical techniques. The main difficulty lies in the divergence of scales as T_c is approached. Large systems paired with a careful finite size analysis are needed and a finite size ansatz and cluster updates or similar techniques are required to overcome the concomitant critical slowing down. For quantum systems, such analyses can be done on bosonic and spin systems [1,2] where lattice Monte Carlo and series expansion techniques allow access to large enough systems to perform a reliable finite size scaling.

The situation for correlated fermionic lattice systems important to condensed matter is different. Analytical solutions only exist for very special setups or weak and strong coupling limits. Semianalytical infinite partial summation techniques [3] can be applied but are in general uncontrolled. Approximate numerical approaches (among

them the dynamical mean field theory (DMFT) [4], which does not include any nonlocal correlations), are known to yield inaccurate critical behavior in two and three dimensions [5,6]. Similarly, large-scale numerical efforts, e.g., diagonalization, lattice quantum Monte Carlo, or large diagrammatic simulations have not yet reached the system sizes necessary to perform a reliable finite size scaling analysis at a critical point. For general systems and parameter regimes, the exponential scaling of these techniques (due to an exponential growth of the Hilbert space or the fermionic sign problem) makes it prohibitively expensive to directly simulate large systems.

Diagrammatic multiscale approaches [7–10] offer an elegant potential remedy to this problem: the difficult correlated part of the system is solved using a nonperturbative many-body method, whereas easier, weakly correlated parts of the problem are subsequently tackled in a perturbative scheme. As perturbation theory generically fails near criticality, it is *a priori* unclear if such a method can accurately describe the behavior near critical points. A first application to the critical properties of the antiferromagnetic phase transition in the three-dimensional Hubbard model in terms of the dynamical vertex approximation (DΓA) [7] has appeared in [11]. This calculation, however, was not fully self-consistent at the two-particle level and required an additional rescaling of the two-particle vertex functions of DΓA introduced in [12,13], resulting in a Gaussian description of the spatial fluctuations characterized by anomalous dimension $\eta = 0$ [11]. The three-dimensional Hubbard model in the infinite interaction strength limit undergoes a continuous classical (i.e., finite temperature) phase transition which is in the universality class of the ϕ^4 theory. The spatial correlations at criticality thus are characterized by $\eta \approx 0.03$ [14] close to

the Gaussian limit $\eta = 0$, which makes it difficult to test if the correct non-mean-field spatial behavior of the interacting system is captured faithfully.

In this Letter we present results for the phase diagram and criticality of a simple fermionic model obtained from a multiscale method that is able to describe non-Gaussian critical behavior. Our multiscale method is the single-site DMFT combined with a dual fermion (DF) approach [8], a diagrammatic expansion in terms of the reducible DMFT vertices. This scheme has previously been shown to have a faster convergence than regular lattice perturbation theories, as it has a small parameter in both the weak- and strong-coupling regimes [15,16]. The starting point of the dual fermion expansion is the nonperturbative DMFT expression for the lattice Green's function [8] and it does not require an *a posteriori* renormalization of vertex functions. We focus on the half-filled Falicov-Kimball (FK) [17] model in two, three and four dimensions. This model arises in various contexts ranging from binary alloys to charge order in intermediate-valence systems and is frequently used to study phase transitions [5]. We choose this model because of its continuous phase transition which at infinite interaction strength is described by a ϕ^4-theory with a Z_2 order parameter [18] which leads to strongly non-Gaussian spatial fluctuations in two dimensions encoded in $\eta = 1/4$, and because of its numerical tractability at the DMFT level [5].

Our results show that non-Gaussian critical behavior in the vicinity of a phase transition and critical exponents can be extracted reliably from diagrammatic multiscale simulations, thereby enabling the use of these methods in more general and more demanding contexts.

Model and method.—We consider the FK model in d dimensions with two types of electrons: heavy, fixed f electrons characterized by a level energy ε_f and the operators $f^{(\dagger)}$ and light, mobile conduction electrons described by the operators $c^{(\dagger)}$ with the dispersion of the hypercubic lattice $\varepsilon_{\mathbf{k}} = -2t \sum_j^d \cos k_j$,

$$\hat{H} = \sum_{\mathbf{k}} \varepsilon_{\mathbf{k}} c_{\mathbf{k}}^\dagger c_{\mathbf{k}} + \sum_i \varepsilon_f f_i^\dagger f_i + U \sum_i c_i^\dagger c_i f_i^\dagger f_i, \quad (1)$$

where U is the interaction strength between c and f electrons. Throughout this paper we will use $t = 1$ as unit of energy.

Within DMFT, the solution of the lattice problem is approximated by a numerically tractable local impurity problem with an effective self-consistently determined hybridization function Δ_ω. The action of the lattice problem (1) in imaginary time is $S = \sum S^{\text{imp}}[c, c^*, n_f] - \sum_{\omega \mathbf{k}} (\Delta_\omega - \varepsilon_k) c_{\omega \mathbf{k}}^* c_{\omega \mathbf{k}}$, where the impurity action S^{imp} reads

$$S^{\text{imp}}[c, c^*, n_f] = \sum_\omega (\Delta_\omega - i\omega - \mu) c_\omega^* c_\omega$$
$$+ \beta(\varepsilon_f - \mu) n_f + U n_f \sum_\omega c_\omega^* c_\omega. \quad (2)$$

Here c_ω, c_ω^* are conduction electron fields at the impurity site, $n_f = 0, 1$ is a classical variable representing the local occupation number of f electrons and $\beta = T^{-1}$ is the inverse temperature. The solution of the single impurity problem (2) can be obtained analytically [19], and in the infinite coordination number limit DMFT yields exact expressions [20,21] for the Green's and vertex functions. We denote the Green's function of the interacting impurity problem as $g_\omega = -\langle c_\omega c_\omega^* \rangle$. The hybridization function Δ_ω is set by taking g_ω equal to the local part of the lattice Green's function $g_\omega = \sum_{\mathbf{k}} G_{\omega \mathbf{k}}^{\text{DMFT}}$. In the FK model, the coupling of the itinerant c electrons to the classical f electrons leads to a separation of the static and dynamic response functions [22], and to a simplified two-frequency (rather than three-frequency) dependence of the two-particle Green's function $\chi_{\omega \omega'} = \langle c_\omega c_\omega^* c_{\omega'} c_{\omega'}^* \rangle$. Moreover, the higher order (three-, four-particle …) impurity vertex functions vanish in the particle-hole symmetric regime of the model (see derivation in Supplemental Material [23]). In the finite dimensional case considered here, DMFT is an approximation and yields a set of mean field exponents for the charge-ordering transition [5].

We then apply our multiscale dual fermion method to obtain nonlocal correlations. Following Ref. [8] we introduce a set of dual fermions ξ, ξ^* and integrate out the original degrees of freedom to rewrite the action of the original lattice problem (1) as

$$\tilde{S} = -\sum_{\omega \mathbf{k}} \xi_{\omega \mathbf{k}}^* [\tilde{G}_{\omega \mathbf{k}}^0]^{-1} \xi_{\omega \mathbf{k}} - \frac{1}{2} \sum_{\omega \omega' j} \gamma_{\omega \omega'} \xi_{\omega i}^* \xi_{\omega i} \xi_{\omega' i}^* \xi_{\omega' i}. \quad (3)$$

Here $\gamma_{\omega \omega'} = g_\omega^{-2} [\chi_{\omega \omega'} - g_\omega g_{\omega'}] g_{\omega'}^{-2}$ is the reducible two-particle vertex of the DMFT impurity problem (2) and $\tilde{G}_{\omega \mathbf{k}}^0 = G_{\omega \mathbf{k}}^{\text{DMFT}} - g_\omega$ denotes the bare dual fermion Green's function.

The dual fermion self-energy is constructed from the reducible DMFT impurity vertex functions. The summation of all of vertex diagrams generates the exact lattice solution but cannot be performed in practice. At this point we therefore resort to a ladder approximation and express the connected part of the dual two-particle Green's function as

$$\tilde{\Gamma}_{\omega \omega'}(\mathbf{q}) = \gamma_{\omega \omega'} - \sum_{\omega''} \gamma_{\omega \omega''} \sum_{\mathbf{k}} \tilde{G}_{\omega'' \mathbf{k}} \tilde{G}_{\omega'' \mathbf{k} + \mathbf{q}} \tilde{\Gamma}_{\omega'' \omega'}(\mathbf{q}). \quad (4)$$

Its zero-order approximation ($\tilde{G} = \tilde{G}^0$) results in DMFT expressions for both the Green's function and the charge susceptibility of the system (see Ref. [24] and Supplemental Material [23]). The dual fermion self-energy $\tilde{\Sigma}_{\omega \mathbf{k}}$ is obtained from $\tilde{\Gamma}_{\omega \omega'}(\mathbf{q})$ via

$$\tilde{\Sigma}_{\omega \mathbf{k}} = \sum_{\mathbf{q}} \tilde{\Gamma}_{\omega \omega}(\mathbf{q}) \tilde{G}_{\omega \mathbf{k} + \mathbf{q}}. \quad (5)$$

Equations (4) and (5) are solved self-consistently. This allows for non-mean-field critical exponents, whereas a
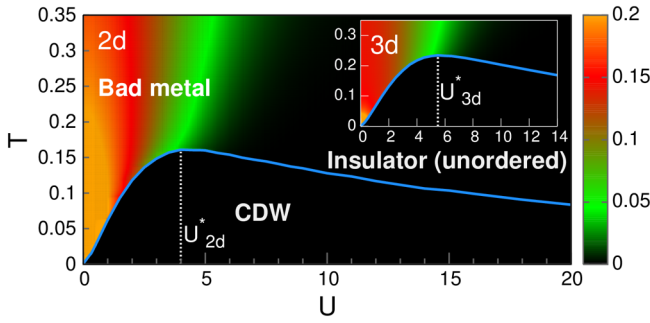
FIG. 1 (color online).   Estimate for the Fermi energy density of
states $A(0) \approx -\beta G_{\text{loc}}(\beta/2)/\pi$ of c electrons in two dimensions,
(inset: three dimensions) as a function of U and T at half-filling.
Solid line $T_c(U)$ indicates a phase transition to the checkerboard
ordered phase (CDW). Above T_c the model shows a crossover
from a metallic phase to the isotropic insulator.

FIG. 2 (color online).   (a) Inverse of static c-electron charge
susceptibility in $d = 2$, 3, 4 as a function of $T - T_c$ at $U = 14$.
(b) Critical exponent γ in $d = 2$, 3, 4 at different values of U for
$U > U^*$. Lines: prediction for Ising universality class, $\gamma = 1.75$ in
two dimensions, 1.24 in three dimensions, 1 in four dimensions.
Error bars represent regression errors. (c) Critical temperatures of the
charge ordering transition in $d = 2$, 3, 4 for different values of U.
Solid lines: DMFT, dimensions indicated on graph. Lines with heavy
symbols: ladder DF. Light symbols: Monte Carlo of Refs [27,28].

finite subset of the diagrams does change T_c but only
results in mean field exponents (see Supplemental Material
[23] and Ref. [25]). The full lattice Green's function
$G_{\omega \mathbf{k}}$ and the lattice two-particle vertex $\Gamma_{\omega \omega' \mathbf{k} \mathbf{k}'}(\mathbf{q})$ can be
obtained from $\tilde{G}_{\omega \mathbf{k}}$ and $\tilde{\Gamma}_{\omega \omega'}(\mathbf{q})$ via $G_{\omega \mathbf{k}} = (\Delta_\omega - \varepsilon_{\mathbf{k}})^{-1} +$
$g_\omega^{-2}(\Delta_\omega - \varepsilon_{\mathbf{k}})^{-2}\tilde{G}_{\omega \mathbf{k}}$ and $\Gamma_{\omega \omega' \mathbf{k} \mathbf{k}'}(\mathbf{q}) = L_{\omega \mathbf{k}} L_{\omega \mathbf{k}+\mathbf{q}} L_{\omega' \mathbf{k}'}$
$L_{\omega' \mathbf{k}'+\mathbf{q}} \tilde{\Gamma}_{\omega \omega'}(\mathbf{q})$, where $L_{\omega \mathbf{k}} = [1 - \tilde{\Sigma}_{\omega \mathbf{k}} g_\omega]^{-1}$. The static
lattice c-electron charge susceptibility becomes $\chi_{cc}(\mathbf{q}) =$
$-T \sum_{\omega \mathbf{k}} G_{\omega \mathbf{k}} G_{\omega \mathbf{k}+\mathbf{q}} + T \sum_{\omega \omega'} \sum_{\mathbf{k} \mathbf{k}'} G_{\omega \mathbf{k}} G_{\omega \mathbf{k}+\mathbf{q}} \Gamma_{\omega \omega' \mathbf{k} \mathbf{k}'}(\mathbf{q})$
$G_{\omega' \mathbf{k}'} G_{\omega' \mathbf{k}'+\mathbf{q}}$.

Results.— We present the phase diagram of the half-
filled FK model on two-dimensional and three-dimensional
cubic lattices obtained in the isotropic phase of the model in
Fig. 1. Shown is our estimate for the c-electron density of
states at Fermi energy ($\omega = 0$) obtained from the DF
calculation as $A(\omega = 0) \approx -\beta G_{\text{loc}}(\beta/2)/\pi$. We find three
different phases: below T_c (indicated by the solid line) a
checkerboard charge-ordered state exists for all values of
U, above T_c the isotropic metallic non-Fermi liquid state
[26] for low U, and a disordered Mott-like insulating state
for large U are separated by a crossover with a character-
istic energy scale U^* indicated by a dashed line in Fig. 1.
At $U > U^*$ a gap in the spectrum is present for all
temperatures and the kinetic energy of the conduction
electrons is small compared to the potential energy and
the phase transition is of second order. At $U < U^*$,
Monte Carlo simulations on finite-size clusters [27,28]
indicate first-order coexistence, whereas DMFT finds an
unconventional continuous phase transition [29,30].

In Figs. 2 and 3 we analyze the critical behavior of the
continuous transition at $U > U^*$. In panel 2(a) we show the
inverse of the static checkerboard $\mathbf{q} = (\pi, \pi, \cdots)$ c-electron
susceptibility χ_{cc} on approach to the charge-ordering phase
transition in two, three, and four dimensions as obtained
from our DF calculations. The divergence of χ_{cc} indicates a
phase transition to the checkerboard charge-ordered phase,
which occurs at half-filling. We find power law behavior
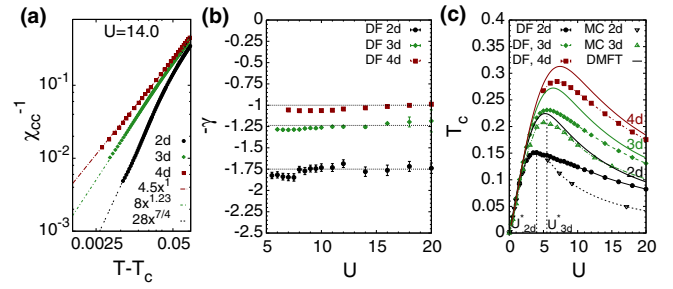for about two decades in $T - T_c$ and χ_{cc}^{-1}, allowing us to fit

the critical exponent γ with good confidence. Panel 2(b)
shows the evolution of γ as a function of U along the
second order line. We observe a significant dimensionality
dependence of γ and an agreement with the Ising univer-
sality class (of the respective dimension) within error bars
for the entire range $U > U^*$. Our error bars reflect the least
square fitting uncertainty for the exponents. In panel 2(c)
we show the critical temperature of the phase transition in
different dimensions as obtained by Monte Carlo simu-
lations [27,28] (obtained on finite-size clusters), DMFT and
dual fermions. Nonlocal correlations in the system lead to a
decrease of the critical temperature from the overestimated
DMFT values towards the Monte Carlo values. The DF
improves on the DMFT for all interaction values studied.
The difference between the dual fermion T_c and the true
transition temperature is determined by all the diagrams not
included in the DF approximation.

In Fig. 3(a) we show the spatial dependence of χ_{cc} along
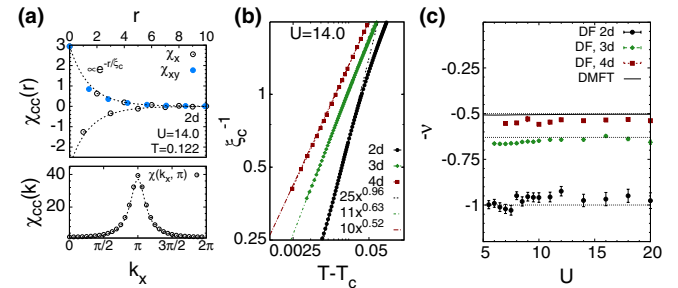the x (open black symbols) and the xy (solid blue symbols)

FIG. 3 (color online).   (a) χ_{cc} as a function of distance (top) along
the x and xy direction, for $U = 14$ and $T = 0.122$. Dashed line:
exponential envelope of χ_{cc}. Bottom: data and fit to Lorentzian in
momentum space for same parameters. (b) Inverse correlation
length ξ^{-1} and power law fit as a function of $T - T_c$ at $U = 14$, for
$d = 2$, 3, 4. (c) Correlation length exponent ν for $d = 2$, 3, 4 along
with theoretical predictions for the Ising model (dashed lines) and
DMFT results (solid line) as a function of U for $U > U^*$.

directions. The spatial modulation of χ_{cc} shows checkerboard ordering, indicated by a change of sign of susceptibility in x-direction. The data are consistent with an exponential decay corresponding to a Lorentzian in momentum space (lower panel), so that we can extract a correlation length ξ. Figure 3(b) shows the critical behavior of ξ as a function of T at $U = 14$, which in agreement with Fig. 2(b) shows a strong dimensionality dependence. The corresponding critical exponent ν, plotted in Fig. 3(c) as a function of U, shows reasonable agreement with the Ising exponents for the entire range of U.

As all critical properties are obtained from the effective action and its derivatives, scaling relations are expected to hold. From γ and ν one therefore can extract the value of $\eta = 2 - \gamma/\nu$ (0.25 in two dimensions, 0.03 in three dimensions), highlighting the correct description of non-Gaussian spatial fluctuations at the phase transition. This result is more general: in the Hubbard model, vertex functions will acquire additional dynamic components, which are absent in the Falicov-Kimball model. However, due to the decoupling of statics and dynamics at a classical phase transition [31], critical exponents only depend on the lattice dimension and the order parameter symmetry and are insensitive to the dynamics of the underlying microscopic model [32]. Correct critical exponents for the Hubbard model may be obtained from an analogous calculation using only static vertex components. In contrast, nonuniversal quantities (e.g., T_c) will depend on dynamic vertex parts and require a more extensive analysis.

We now turn to a discussion of the electronic properties that underlie this behavior. Figure 4(a) shows the local fc occupancy $n_{fc} = \langle c^\dagger c f^\dagger f \rangle_{\text{loc}}$ in two dimensions and our estimate for the local density of states as a function of U near the crossover between metallic and insulating states at $T > T_c$. DMFT calculations [30] showed continuous crossover behavior and no hysteresis for both quantities. Nonlocal correlations do not change this behavior qualitatively, but we find that the crossover scale U^* is slightly smaller than in DMFT. We also find, consistent with expectation, that deviations from the DMFT results are largest near the point where the curve is closest to the phase transition to the ordered state and critical phenomena become important. Away from this region, DF and DMFT results are remarkably similar and nonlocal correlations appear less important.

The momentum-resolved spectral function estimates shown in panels (b) and (c) of Fig. 4 highlight this further. DF (main panels) and DMFT (insets) DOS at the Fermi energy are shown as a function of momentum for $U = 4$ and $U = 1$. The temperature is chosen to be just above T_c for $U = 4$. The weak correlation regime deep within the phase at $U = 1$ is well captured by the momentum-independent DMFT self energy. Near T_c at $U = 4$, the deviations between the DF and DMFT solutions become substantial. DMFT shows a comparatively large and k-independent spectral function in a large area around
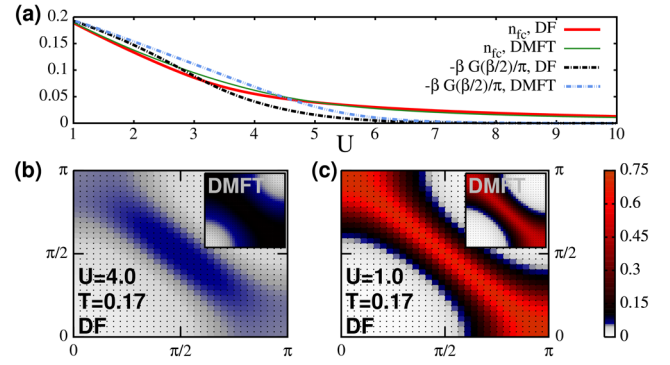

FIG. 4 (color online). (a) fc occupancy n_{fc} (solid lines) and local density of states (DOS) estimate at the Fermi energy, $A(\omega = 0) \approx -\beta G_{\text{loc}}(\beta/2)/\pi$, (dashed lines) in two dimensions as a function of U in DMFT and DF, both showing a smooth crossover from metal to Mott-like insulator. Bottom: Momentum-resolved $-\beta G_k(\beta/2)$ for $U = 4.0$ (b) and $U = 1.0$ (c), as obtained in DF (main panel) and DMFT (insets). Black dots indicate the mesh points on which DF and DMFT are evaluated.

the noninteracting Fermi surface. DF, in contrast, exhibits a much narrower and nontrivial momentum dependent spectral function that suppresses the density of states near the $(\pi, 0)$ and $(0, \pi)$ points but not near the zone diagonal $(\pi/2, \pi/2)$ points. This behavior is expected because a divergence in the two-particle propagator feeds back into the single-particle Green's function through Eq. (5). The effect is reminiscent of the momentum-selective pseudogap regime in the Hubbard model, where both short ranged correlations contained in, e.g., cluster DMFT [33] or long ranged correlations contained in DF and DΓA calculations [13,15,16] result in qualitatively similar behavior.

The charge order phase transition in this model persists away from half filling [34]. Figure 5(a) shows T_c as a function of c-electron chemical potential for three different f-electron concentrations. We find that doping suppresses T_c both in DMFT (open symbols) and DF (filled symbols), with the DF T_c always below DMFT. Panel (b) shows the evolution of the c-electron density as a function of c-electron chemical potential at T_c. The large difference between DF and DMFT results is a consequence of correlation effects absent in DMFT.
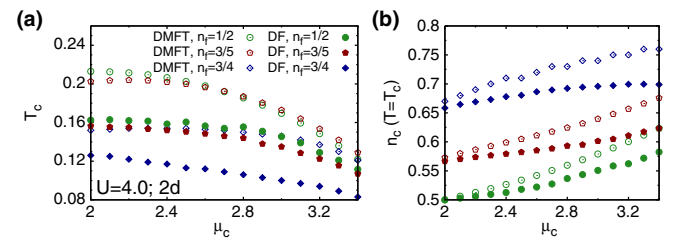

FIG. 5 (color online). (a) Transition temperature T_c and (b) average occupation number of c electrons at $T = T_c$ as a function of c-electron chemical potential in two dimensions at $U = 4$ at an average f electron occupation number of $n_f = 1/2; 3/5; 3/4$. DMFT results: open symbols. DF: filled symbols.

Summary.—In conclusion, we have applied the "dual fermion" diagrammatic multiscale method to an interacting quantum many-body system. We demonstrated that our dual fermion ladder approximation recovers the exact interacting critical behavior in $d = 2$, 3, 4 dimensions and that diagrammatic multiscale methods can yield accurate results for the criticality of interacting fermionic lattice models. We also showed that the method provides valid results away from particle-hole symmetry. It may therefore be able to provide accurate predictions for more complicated (and in particular frustrated) models [35], where no reliable theoretical tools are available so far, as well as for transport properties near and far from equilibrium [36,37]. It also motivates the use of multiscale methods to gain insight into critical phenomena that are far less clear, such as the superconducting transition in the cuprates [38] and the quantum melting of magnetism in certain heavy fermion compounds [39], where many continuous quantum phase transitions appear to be beyond the traditional classification scheme [40,41].

---

*aantipov@umich.edu
†egull@umich.edu
‡kirchner@pks.mpg.de

[1] H. G. Evertz, G. Lana, and M. Marcu, Phys. Rev. Lett. **70**, 875 (1993).

[2] B. Capogrosso-Sansone, S. G. Söyler, N. Prokof'ev, and B. Svistunov, Phys. Rev. A **77**, 015602 (2008).

[3] N. E. Bickers, in *Theoretical Methods for Strongly Correlated Electrons*, CRM Series in Mathematical Physics, edited by D. Senechal, A.-M. Tremblay, and C. Bourbonnais (Springer, New York, 2004) p. 237.

[4] A. Georges, G. Kotliar, W. Krauth, and M. J. Rozenberg, Rev. Mod. Phys. **68**, 13 (1996).

[5] J. Freericks and V. Zlatić, Rev. Mod. Phys. **75**, 1333 (2003).

[6] P. Anders, E. Gull, L. Pollet, M. Troyer, and P. Werner, New J. Phys. **13**, 075013 (2011).

[7] A. Toschi, A. A. Katanin, and K. Held, Phys. Rev. B **75**, 045118 (2007).

[8] A. N. Rubtsov, M. I. Katsnelson, and A. I. Lichtenstein, Phys. Rev. B **77**, 033101 (2008).

[9] C. Slezak, M. Jarrell, T. Maier, and J. Deisz, J. Phys. Condens. Matter **21**, 435604 (2009).

[10] C. Taranto, S. Andergassen, J. Bauer, K. Held, A. Katanin, W. Metzner, G. Rohringer, and A. Toschi, arXiv:1307.3475.

[11] G. Rohringer, A. Toschi, A. Katanin, and K. Held, Phys. Rev. Lett. **107**, 256402 (2011).

[12] K. Held, A. A. Katanin, and A. Toschi, Prog. Theor. Phys. Suppl. **176**, 117 (2008).

[13] A. A. Katanin, A. Toschi, and K. Held, Phys. Rev. B **80**, 075104 (2009).

[14] C. Holm and W. Janke, Phys. Rev. B **48**, 936 (1993).

[15] A. N. Rubtsov, M. I. Katsnelson, A. I. Lichtenstein, and A. Georges, Phys. Rev. B **79**, 045133 (2009).

[16] H. Hafermann, G. Li, A. N. Rubtsov, M. I. Katsnelson, A. I. Lichtenstein, and H. Monien, Phys. Rev. Lett. **102**, 206401 (2009).

[17] L. Falicov and J. Kimball, Phys. Rev. Lett. **22**, 997 (1969).

[18] T. Kennedy and E. H. Lieb, Physica (Amsterdam) **138A**, 320 (1986).

[19] U. Brandt and C. Mielsch, Z. Phys. B **75**, 365 (1989).

[20] W. Metzner and D. Vollhardt, Phys. Rev. Lett. **62**, 324 (1989).

[21] V. Zlatic and B. Horvatic, Solid State Commun. **75**, 263 (1990).

[22] J. K. Freericks and P. Miller, Phys. Rev. B **62**, 10022 (2000).

[23] See Supplemental Material at http://link.aps.org/supplemental/10.1103/PhysRevLett.112.226401 for detailed DMFT and dual fermion formulation and comparison of different approximations.

[24] H. Hafermann, F. Lechermann, A. N. Rubtsov, M. I. Katsnelson, A. Georges, and A. I. Lichtenstein, in Modern Theories of Many-Particle Systems in Condensed Matter Physics, Lecture Notes in Physics, Vol. 843, edited by D. C. Cabra, A. Honecker, and P. Pujol (Springer-Verlag, Berlin, 2012) p. 145.

[25] S. Brener, H. Hafermann, A. N. Rubtsov, M. I. Katsnelson, and A. I. Lichtenstein, Phys. Rev. B **77**, 195105 (2008).

[26] Q. Si, G. Kotliar, and A. Georges, Phys. Rev. B **46**, 1261 (1992).

[27] M. M. Maśka and K. Czajka, Phys. Rev. B **74**, 035109 (2006).

[28] M. Žonda, P. Farkašovský, and H. Čenčariková, Solid State Commun. **149**, 1997 (2009).

[29] J. K. Freericks and R. Lemanski, Phys. Rev. B **61**, 13438 (2000).

[30] P. G. J. van Dongen, Phys. Rev. B **45**, 2267 (1992).

[31] V. Popov, *Functional Integrals in Quantum Field Theory and Statistical Physics* (Kluwer, Dordrect, 1983).

[32] K. Wilson and M. Fisher, Phys. Rev. Lett. **28**, 240 (1972).

[33] E. Gull, O. Parcollet, P. Werner, and A. J. Millis, Phys. Rev. B **80**, 245102 (2009).

[34] R. Lemanski, J. K. Freericks, and G. Banach, Phys. Rev. Lett. **89**, 196403 (2002).

[35] G. Li, A. E. Antipov, A. N. Rubtsov, S. Kirchner, and W. Hanke, Phys. Rev. B **89**, 161118 (2014).

[36] E. Muñoz, C. J. Bolech, and S. Kirchner, Phys. Rev. Lett. **110**, 016601 (2013).

[37] V. Zlatić and J. K. Freericks, Phys. Rev. Lett. **109**, 266601 (2012).

[38] V. Mishra, U. Chatterjee, J. C. Campuzano, and M. R. Norman, Nat. Phys. **10**, 357 (2014).

[39] Q. Si and F. Steglich, Science **329**, 1161 (2010).

[40] Q. Si, J. H. Pixley, E. Nica, S. J. Yamamoto, P. Goswami, R. Yu, and S. Kirchner, J. Phys. Soc. Jpn. **83**, 061005 (2014).

[41] O. Stockert, S. Kirchner, F. Steglich, and Q. Si, J. Phys. Soc. Jpn. **81**, 011001 (2012).

[42] TRIQS, http://ipht.cea.fr/triqs/.